

# Duplex Mechanism of TiC Formation and Ti Dissolution Behavior in KCl-LiCl Molten Salt

H. Nadimi, H. Sarpoolaky, M. Soltanieh\*

\* Mansour\_soltanieh@iust.ac.ir

School of Metallurgy and Materials Engineering, Iran University of Science and Technology, Narmak, Tehran, 16846-13114, Iran

Received: July 2023

Revised: October 2023

Accepted: October 2023

DOI: 10.22068/ijmse.3322

**Abstract:** In the present investigation, an attempt was made to evaluate the dissolution behavior of Ti in molten KCl-LiCl. The X-ray diffraction (XRD) pattern of a heated Ti plate at 800°C for 4 h without carbon black in molten salt revealed that TiCl<sub>3</sub> formation was feasible. For more assurance, the Ti plate was heated at 950°C for 4 h in the presence of carbon black to identify synthesized TiC. Transmission electron microscope (TEM) and scanning electron microscope (SEM) images from precursors and the final product showed that nano-crystalline TiC formation from coarse Ti particles was almost impossible without Ti dissolution. Thermodynamics calculations using Factsage software proved that it was possible to form various TiCl<sub>x</sub> compounds. The TiC formation mechanism can be discussed in two possible ways: a reaction between Ti ion and carbon black for synthesizing TiC (direct) and a reaction between TiCl<sub>4</sub> and carbon black led to indirect TiC synthesis. Elemental mapping using energy dispersive X-ray spectroscopy (EDS) indicated that up to 815°C, chlorine existed in the map.

**Keywords:** Molten salt synthesis, Ti dissolution, Mechanism, TiC.

## 1. INTRODUCTION

The molten salt synthesis method was identified as a trustworthy, practical, and innovative route for TiC synthesis. Increasing reactants contact surface, helping the species dissolution, decreasing synthesis temperature and duration, the non-agglomerated final product, and user-friendly method were a small part of the reliable features of the molten salt method compared to other methods [1-5]. The TiC synthesis either as bulk or as a coating needs sufficient dissolution and mobility of species which were provided by proper molten salt [6, 7]. Taking into account the properties of each salt such as viscosity, wettability, working temperature range, etc., led to promoting the efficiency of TiC synthesis [8, 9]. Choosing a salt with a high viscosity caused to decline in the rate of Ti transfer to the surface of the carbon. Among the chloride salts, KCl and LiCl had the lowest viscosity [10]. Baumli et al. [11] demonstrated that by increasing the cation radius of chloride salt, the graphite wettability would improve.

The dissolution behavior study of metals in the molten salt is a key point for mechanism determination. Liu et al [12] showed that from elemental V and acetylene black powders in the presence of molten NaCl-KCl, V<sub>2</sub>C can be

fabricated as the main phase but lack of molten salt led to production by-products such as V, VC, and V<sub>2</sub>O<sub>3</sub>. They suggested that the dissolution of V in molten salt promoted the V<sub>2</sub>C formation. Wang et al. [13] indicated that the dissolution of Cr and subsequently Cr(II) formation in a salt medium, improve the formation of Cr<sub>2</sub>AlB<sub>2</sub>. Ti dissolution behavior in Cl-based salt has remained vague so far. Therefore, some investigations were conducted to distinguish the role of chloride salts on Ti dissolution. Kreye et al. [14] showed that Ti powders dissolved partially in NaCl-KCl salt which led to TiCl<sub>2</sub> and TiCl<sub>3</sub> formation. Straumantis et al. [15] fabricated Ti coating on the surface of Fe in the KCl and NaCl molten salts. Increasing the temperature above 910°C Ti diffuses to the substrate which is due to the dissolution of Ti. Shurov et al. [16] proved that Li could be dissolved in LiCl salt which was recognized as ionic-electronic melt and dissociated to cations and delocalized electrons.

The TiC synthesis mechanism in the molten salt medium was investigated by various researchers. Li et al. [17] suggested that TiC coating could be synthesized in the reaction between Ti ions and carbon. Based on their findings, a direct reaction between Ti powder and carbon results in a non-dense coating on the surface of the diamond. Liu

et al. [18] expressed that the transfer of Ti to the surface of graphite plays an important role in mechanism prediction. The direct transfer of Ti solid particles and the transfer of dissolved Ti were two potential routes for TiC formation. Yang et al. [19] represented that the direct synthesis of TiC with 50 nm in average size from Ti with particle size about 45  $\mu\text{m}$  was impossible in practice, therefore, it was supposed that various Ti species would form at first and then TiC would synthesis completely.

In the present study, an attempt was made to predict the synthesis pathway of TiC formation using KCl-LiCl eutectic composition from two potential routes, i.e. direct and indirect ways. The dissolution behavior of the Ti element in the KCl-LiCl salt medium was investigated by applying XRD patterns. The thermodynamics assessment of all happened reactions in the path of TiC synthesis was surveyed using Factsage software.

## 2. EXPERIMENTAL PROCEDURES

Elemental Ti and carbon black were used as starting materials for TiC synthesis with a molar ratio equal to 1:1. The eutectic composition from KCl and LiCl salts with purity greater than 99% was mixed with precursors which weight ratio of salt to reactants was chosen equal to 9:1. The mixture was blended for 45 mins by agate in a mortar and then was heated in an oven for 60 mins at 110°C for omitting water. The dried sample was placed in an alumina crucible and was heated at 800 and 950°C for 4 h under the protection of purified Ar gas (99.999%). The synthesized product was cooled in the furnace and after that was washed using hot distilled water five times. Eventually, the final powder was separated from the salt by the filter paper at room temperature. The synthesized samples were analyzed by X-ray diffraction (Bruker D8 advance) equipped with Cu-K $\alpha$  radiation in the range of 20° < 2 $\theta$  < 90°, and therefore, the phases were identified using X'Pert HighScore software. To examine the morphology of reactants and synthesized TiC, the microscopic images were taken by transmission electron microscope (EM208S PHILIPS 100 kV) and scanning electron microscope (FEI ESEM QUANTA 200). The elemental mapping was conducted using energy-dispersive X-ray spectroscope (EDS Silicon Drift 2017) analysis. The X-ray fluorescence (PHILIPS PW 1480) was

applied for elemental analysis.

## 3. RESULTS AND DISCUSSION

### 3.1. Ti Dissolution Behavior in Molten KCl-LiCl

To investigate the dissolution behavior of Ti in KCl-LiCl molten salt, some similar Ti plate pieces (10 mm  $\times$  10 mm) were mixed with the eutectic composition of KCl-LiCl in the absence of carbon powder and placed in an alumina crucible equipped with a lid. The mixture was heated at 800°C for 4 h. The XRD pattern of the heated mixture without washing with hot distilled water is depicted in Fig. 1. According to Fig. 1, five peak series are visible in this pattern that is related to KCl and LiCl salts, TiCl<sub>3</sub>, Li<sub>2</sub>O<sub>2</sub>, and Ti<sub>x</sub>O<sub>y</sub>. KCl and LiCl are highly soluble salts in the water and because the final product doesn't wash with water, their peaks are visible in the diffraction pattern. The most important phase which is diffracted in this Fig. is the TiCl<sub>3</sub> phase. Based on observation after completing the heating process, no traces of Ti plates were found in the crucible. On the other hand, no peaks of elemental Ti were observed in this diffraction pattern. These reasons prove that Ti plates participate in a chemical reaction. The melting and boiling points of Ti are 1668 and 3287°C, respectively. Hence, the Ti element doesn't undergo any phase transformation during heating up to 800°C.

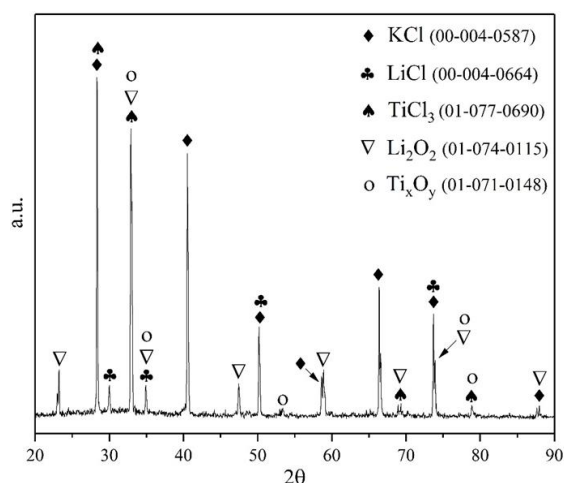
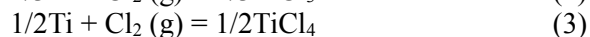
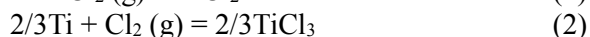


**Fig. 1.** XRD pattern of heated Ti plates in contact with KCl-LiCl salt in the absence of carbon black at 800°C for 4 h before washing with hot distilled water.

Therefore, based on in XRD pattern, the TiCl<sub>3</sub> phase forms from a reaction between Ti ions and

ionized chlorine in the molten salt. This result follows the findings obtained in the previous research [14]. Based on Factsage software calculations, the  $\text{TiCl}_x$  various compounds formation possibility is investigated according to Fig. 2. Three various compounds such as  $\text{TiCl}_2$ ,  $\text{TiCl}_3$ , and  $\text{TiCl}_4$  can be formed as follows:



Based on Fig. 2, the  $\Delta G$  value for all compounds is negative which shows these reactions progress spontaneously. Therefore, there is no thermodynamic limitation for the formation of these three chlorides. It is worthy of note that according to Factsage data, with increasing the temperature to  $829^\circ\text{C}$ ,  $\text{TiCl}_3$  converts from solid to gas state. Also, with increasing the temperature up to  $135^\circ\text{C}$ ,  $\text{TiCl}_4$  is at liquid state but, over this temperature changes to a gaseous state.

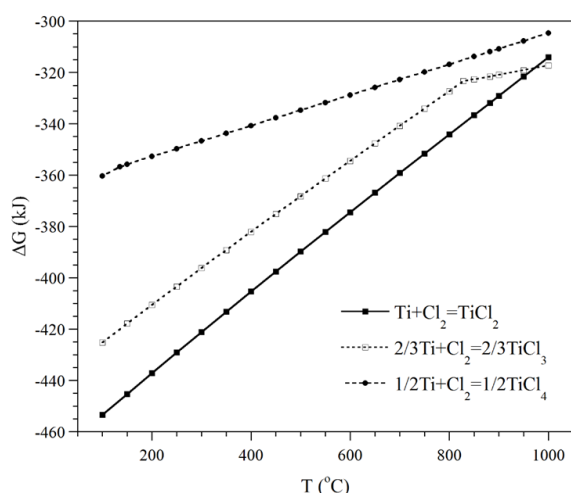
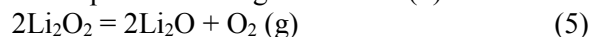


Fig. 2. Ellingham diagram for formation of  $\text{TiCl}_2$ ,  $\text{TiCl}_3$  and  $\text{TiCl}_4$ .

$\text{Ti}_x\text{O}_y$  as an unpleasant phase appears in the XRD pattern. The oxygen entering the heating chamber accompanied by purified Ar is an inevitable problem that causes Ti oxidation. Because the dissolution of  $\text{Ti}_x\text{O}_y$  in chloride salt is very difficult, at first, Ti plates dissolve in the salt, and secondly, a reaction happens between Ti ion and  $\text{O}_2$ . This is another clue that shows that Ti plates dissolve in KCl-LiCl salt.  $\text{Li}_2\text{O}_2$  is the last phase that diffracts in the XRD pattern. The formation of this compound is another reason for the ionization of salts with increasing temperatures. In general, the reaction between  $\text{O}_2$  and Li led to  $\text{Li}_2\text{O}$  formation based on the reaction (4):

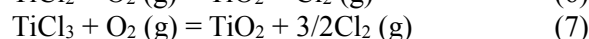
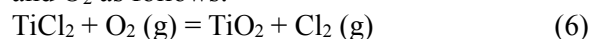


The  $\Delta G$  value of reaction (4) is negative, accordingly, there is no obstacle for  $\text{Li}_2\text{O}$  formation. But, in lower temperatures  $\text{Li}_2\text{O}_2$  forms that with increasing temperature decompose according to reaction (5):



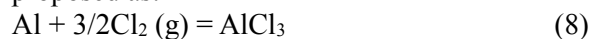
Based on Factsage software, up to a temperature around  $150^\circ\text{C}$ , the value of  $\Delta G$  is positive, hence the  $\text{Li}_2\text{O}_2$  is a stable phase. When the temperature rises to higher values, the reaction (5) progresses to the right spontaneously. Therefore, with increasing temperatures above  $150^\circ\text{C}$ ,  $\text{Li}_2\text{O}_2$  recognised as a stable phase. Because the XRD analysis is conducted on the cooled sample until room temperature, the  $\text{Li}_2\text{O}_2$  peaks are visible in the XRD pattern, according to Fig. 1.

For more assurance about  $\text{TiCl}_x$  formation, three samples were synthesized at  $750$ ,  $815$ , and  $950^\circ\text{C}$  for 4 h. The Cl elemental mapping from the final product without washing with water was illustrated in Fig. 3. Two important points can be extracted from Fig., 1) at  $750$  and  $815^\circ\text{C}$  Cl element can be seen clearly in the map, but with increasing the temperature to  $950^\circ\text{C}$ , there is no sign of Cl was observed in the map (not shown in this paper), 2) by increasing the temperature from  $750$  to  $815^\circ\text{C}$ , the density of Cl in the elemental map decrease drastically. The formed  $\text{TiCl}_x$  can be subjected to contact with oxygen in the synthesis chamber that leads to a reaction between  $\text{TiCl}_x$  and  $\text{O}_2$  as follows:



The  $\Delta G$  value of these reactions is negative, therefore there is no obstacle to  $\text{TiO}_2$  and  $\text{Cl}_2$  formation. In the previous study [1], it is shown that  $\text{TiO}_2$  formation during TiC synthesis under the protection of Ar gas unavoidable problem. These reactions are a reason for eliminating  $\text{TiCl}_x$  at elevated temperatures.

The other reason will be explained in the following section. To examine the role of produced chlorine gas, a crucible without the lid is placed in the synthesis chamber and the experiments are repeated several times. Based on observations, the upper Al flange undergoes corrosion. The XRF analysis from this section indicates that chlorine exists in the corroded section. The possible reaction is proposed as:



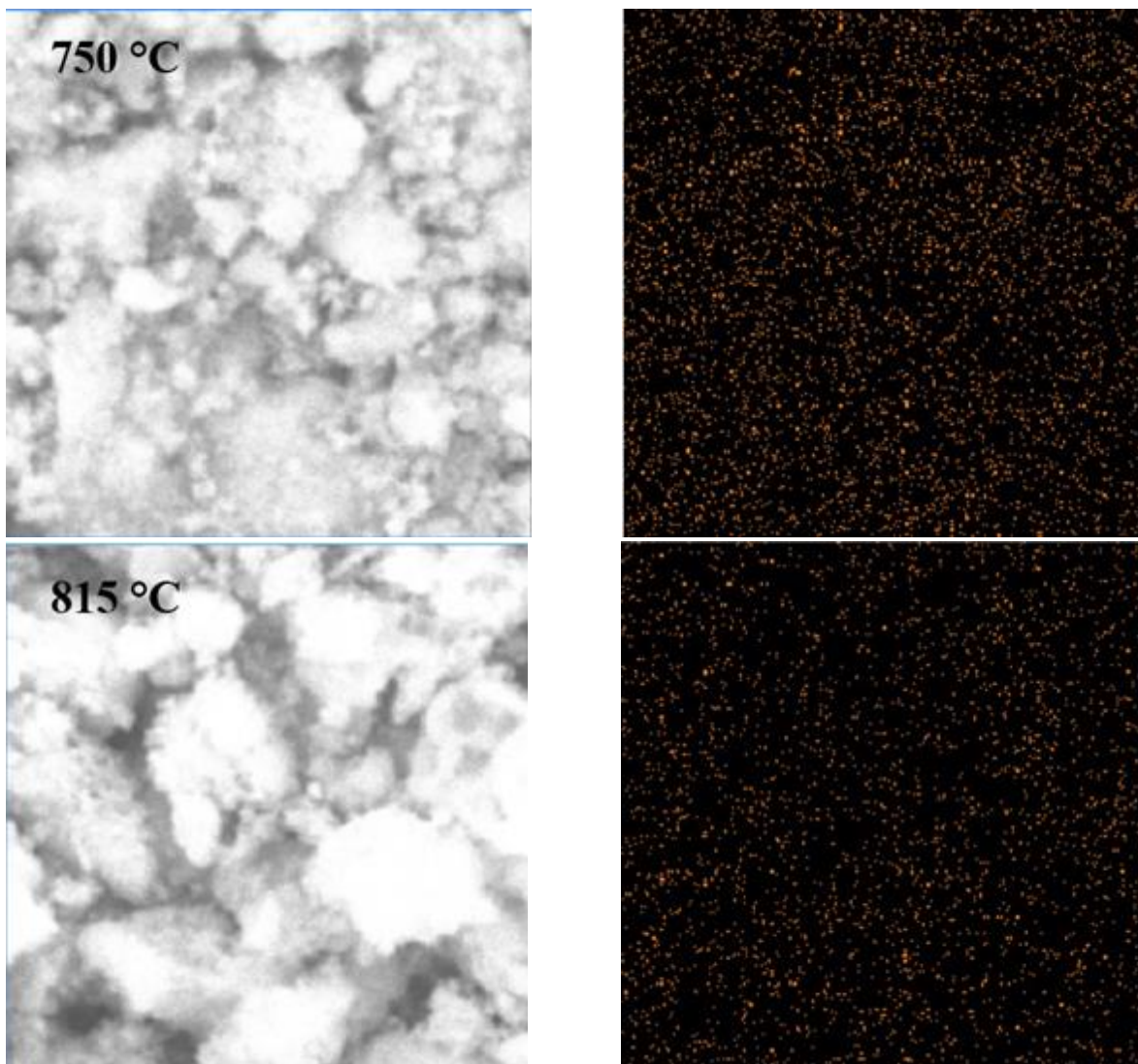


**Fig. 3.** Chlorine elemental mapping using EDS analysis at 750 and 815°C.

To examine Ti dissolution on TiC synthesis, Ti plates were heated in the presence of carbon black at 950°C for 4 h. The XRD pattern of the synthesized TiC is depicted in Fig. 4. As seen in Fig. 4, all sharp and narrow peaks in the pattern are related to TiC without remaining any trace of starting materials. This phenomenon shows that Ti plates dissolve in molten KCl-LiCl and then react with carbon black to produce pure TiC.

### 3.2. The Direct Mechanism of TiC Synthesis in Molten KCl-LiCl

It is shown that the TiC synthesis mechanism in KCl-LiCl molten salt conforms to the "template growth" route [1, 20]. Comparing the particle size of the reactants and the final product is useful for proving this claim.

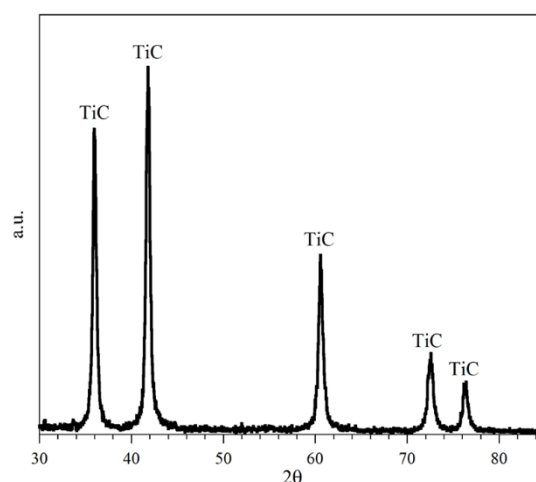


**Fig. 4.** XRD pattern of synthesized TiC in contact with KCl-LiCl salt in the presence of carbon black at 950°C for 4 h.

The morphology of reactants and synthesized TiC are illustrated in Fig. 5. In Fig. 5 a, an individual Ti particle is visible with an average size of less than 100  $\mu\text{m}$  the shape of this particle is irregular. The TEM image of carbon black which is depicted in Fig. 5 b shows that the average size of a globular carbon black is about 70 nm. The average size of the synthesized TiC particle following Fig. 5 c taken by TEM, is about 20 nm. Therefore, a nano-size particle can't be produced from a micro-size one. A key point for investigating the synthesis mechanism is how Ti particles transfer to the surface of an individual carbon black. There are two possible modes for this transfer: 1) Ti particles move to the surface of carbon black directly, and 2) a portion of Ti particles dissolve in the molten KCl-LiCl salt and afterwards transfer to the surface of the carbon. In the first mode, Ti particles must be small enough

not to settle to the bottom of the crucible. On the other hand, for an acceptable contact between Ti and carbon, Ti particles must be fine to achieve a homogenous TiC bulk.

In this research, a nano-size TiC is synthesized from micro-size Ti powders, therefore, if TiC is synthesized through the first mode, TiC particles will fabricate in micro-scale which is in contrast to the Fig. 5 c. As a result, Ti coarse particles dissolve in the molten salt medium and therefore transfer to the surface of carbon black.

The direct mechanism for TiC synthesis is proposed as follows: the dissolution of Ti particles in the molten salt leads to the formation of Ti(II) and Ti(III) ions. An in-situ reaction happens between Ti and carbon by transferring Ti(II) ion to the outer surface of carbon black, according to reaction (9):

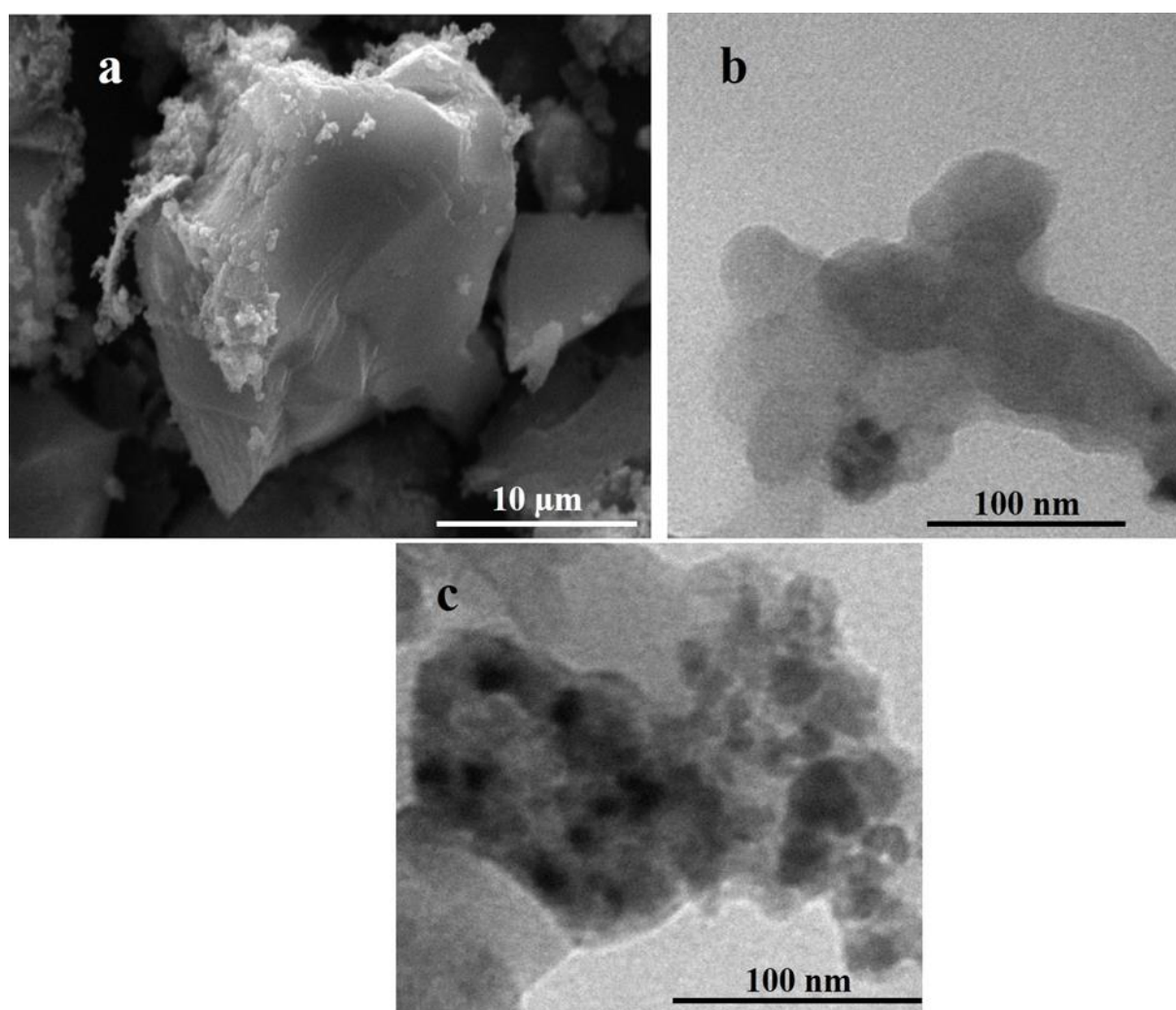
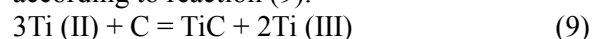


Fig. 5. Microscopic images of a) Ti, b) C and c) synthesized TiC.

The produced Ti(III) ions move to the salt medium and are exposed to Ti powders. A reaction between Ti(III) and Ti occurs according to reaction (10):



By reproducing Ti(II) ions and transferring them to the surface of carbon, the TiC synthesis reaction takes place again. Finally, molten salt is depleted from Ti powders. The  $\Delta G$  value for TiC formation from elemental reactants is illustrated in Fig. 6. Based on Fig. 6, the negative value for  $\Delta G$  shows that this reaction takes place to the right.

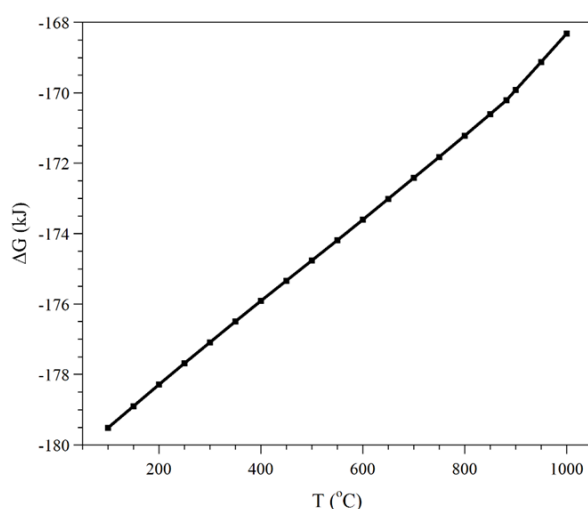
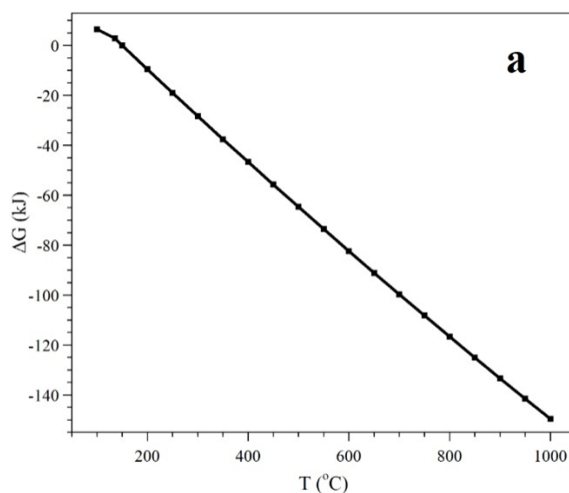


Fig. 6. Gibbs free energy for TiC direct formation from elemental Ti and carbon.

### 3.3. Indirect Mechanism of TiC Synthesis in Molten KCl-LiCl

It was specified in section 3.1 that the  $\text{TiCl}_x$  formation is feasible in the KCl-LiCl medium.



Accordingly, in an indirect way, the formed  $\text{TiCl}_2$  reacts with carbon black, and TiC is produced as follows:



The produced  $\text{TiCl}_4$  gas is in contact with Ti powders that result in  $\text{TiCl}_2$  formation:



The Gibbs free energy of reactions (11) and (12) is depicted in Fig. 7 using Factsage software. According to Fig. 7 a, with increasing the temperature to about  $200^\circ\text{C}$ , the  $\Delta G$  value is positive, therefore reaction (11) moves in the opposite direction. This means that TiC formation up to  $200^\circ\text{C}$  is impossible in practice. In the previous study [1, 6], it was shown that TiC nucleation starts at  $700^\circ\text{C}$ . When the temperature rises above  $200^\circ\text{C}$ , the  $\Delta G$  tends to have negative values, which causes the TiC formation according to the reaction (11). Based on Fig. 7 b, the  $\text{TiCl}_2$  phase forms at any temperature due to the  $\Delta G$  value. Based on reaction (12), the reproduction of  $\text{TiCl}_2$  is useful for TiC formation, because it can participate in the reaction (11) again.

## 4. CONCLUSIONS

The dissolution behavior of the Ti plate is investigated in molten KCl-LiCl salt. The XRD pattern of the heated sample at  $800^\circ\text{C}$  for 4 h shows that the  $\text{TiCl}_3$  phase can be fabricated in the salt medium. The molten salt accelerates the dissolution of Ti plates that resulting in introducing Ti ions to the salt medium. The role of Ti ions in TiC synthesis is more than Ti powders. The estimation of the TiC synthesis mechanism is studied through two potential routes.

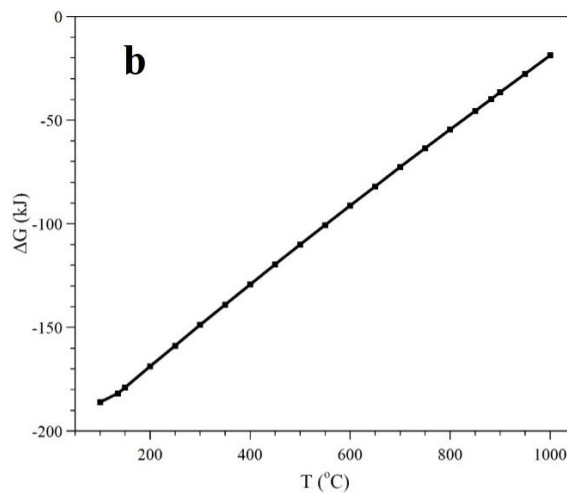


Fig. 7. Gibbs free energy for a) TiC and b)  $\text{TiCl}_2$  formation.

In first way, the reaction of Ti (II) ion and carbon causes to formation of TiC powder. In a second way, a reaction between  $\text{TiCl}_2$  and carbon black leads to TiC formation indirectly. The microscopic images of the final product and reactants show that the synthesis of nano-size TiC from micro-size Ti is impossible without the dissolution of Ti.

## REFERENCES

- [1]. Nadimi, H., Soltanieh, M. and Sarpoolaky, H., "The formation mechanism of nanocrystalline TiC from KCl–LiCl molten salt medium." *Ceram. Int.*, 2020, 46, 18725-18733.
- [2]. Cao, C., Liu, W., Javadi, A., Ling, H. and Li, X., "Scalable manufacturing of 10 nm TiC nanoparticles through molten salt reaction." *Procedia Manuf.*, 2017, 10, 634-640.
- [3]. Huang, Z., Li, F., Jiao, C., Liu, J., Huang, J., Lu, L., Zhang, H. and Zhang, S., "Molten salt synthesis of  $\text{La}_2\text{Zr}_2\text{O}_7$  ultrafine powders." *Ceram. Int.*, 2016, 42, 6221-6227.
- [4]. Li, M., Zhou, D., Li, C. P. and Zhao, Z., "Low temperature molten salt synthesis of YAG: Ce spherical powder and its thermally stable luminescent properties after post-annealing treatment." *Mater. Sci. in Semicond. Process.*, 2016, 44, 101-107.
- [5]. Gupta, S. K. and Mao, Y., "A review on molten salt synthesis of metal oxide nanomaterials: Status, opportunity, and challenge." *Prog. Mater. Sci.*, 2021, 117, 100734.
- [6]. Nadimi, H., Sarpoolaky, H. and Soltanieh, M., "Formation reaction kinetics of nanocrystalline TiC via molten LiCl–KCl applying the shrinking core model." *Ceram. Int.*, 2021, 47, 12859-12869.
- [7]. Behboudi, F., Kakroudi, M. G., Vafa, N. P. and Faraji, M., "Molten salt synthesis of in-situ TiC coating on graphite flakes." *Ceram. Int.*, 2021, 47, 8161-8168.
- [8]. Li, Z., Zhang, S. and Lee, W. E., "Molten salt synthesis of zinc aluminate powder." *J. Eur. Ceram. Soc.*, 2007, 27, 3407-3412.
- [9]. Bao, K., Wen, Y., Khangkhamano, M. and Zhang, S., "Low-temperature preparation of titanium diboride fine powder via magnesiothermic reduction in molten salt." *J. Am. Ceram. Soc.*, 2017, 100, 2266-2272.
- [10]. Janz, G. J., Yamamura, T. and Hansen, M. D., "Corresponding-states data correlations and molten salts viscosities." *Int. J. Thermophys.*, 1989, 10, 159-171.
- [11]. Baumli, P. and Kaptay, G., "Wettability of carbon surfaces by pure molten alkali chlorides and their penetration into a porous graphite substrate." *Mater. Sci. Eng. A*, 2008, 495, 192-196.
- [12]. Liu, R. J., Yang, L. X., Wang, Y., Liu, H. J., Zhu, S. L. and Zeng, C. L., "Synthesis and characterization of submicron-sized  $\text{V}_2\text{AlC}$  ceramics by a two-step modified molten salt method." *Ceram. Int.*, 2021, 47, 16086-16093.
- [13]. Wang, Y., Yang, L. X., Liu, R. J., Liu, H. J., Zeng, C. L., Zhu, S.L. and Fu, C., "Ternary-layered  $\text{Cr}_2\text{AlB}_2$  synthesized from Cr, Al, and B powders by a molten salt-assisted method." *Powder Technol.*, 2021, 387, 354-362.
- [14]. Kreye, W. C. and Kellogg, H. H., "The Equilibrium between Titanium Metal,  $\text{TiCl}_2$ , and  $\text{TiCl}_3$  in NaCl-KCl Melts." *J. Electrochem. Soc.*, 1957, 104, 504.
- [15]. Straumanis, M. E., Shih, S. T. and Schlechten A. W., "The mechanism of deposition of titanium coatings from fused salt baths." *J. Electrochem. Soc.*, 1957, 104, 17.
- [16]. Shurov, N. I., Anfinogenov, A.I., Chebykin, V. V., Klevtsov, L. P. and Kazanskii, E. G. *Refractory Metals in Molten Salts, Their Chemistry, Electrochemistry and Technology*, 1<sup>st</sup>. ed. Kerridge, D. H. and Polyakov, E. G. NATO ASI Series, vol 53. Springer, Dordrecht, 1998, 81-86.
- [17]. Li, C. H., Lu, H. B., Xiong, W. H. and Chen, X., "Diamond and graphite coated with polyalloys by an immersion method." *Surf. Coat. Technol.*, 2002, 150, 163-169.
- [18]. Liu, X., Wang, Z. and Zhang, S., "Molten salt synthesis and characterization of titanium carbide-coated graphite flakes for refractory castable applications." *Int. J. Appl. Ceram. Technol.*, 2011, 8, 911-919.
- [19]. Yang, L., Wang, Y., Liu, R., Liu, H., Zhang, X., Zeng, C. and Fu, C., "In-situ synthesis of nanocrystalline TiC powders,

- nanorods, and nanosheets in molten salt by disproportionation reaction of Ti (II) species." *J. Mater. Sci. Technol.*, 2020, 37, 173-180.
- [20]. Dong, Z. J., Li, X. K., Yuan, G. M., Cong, Y., Li, N., Jiang, Z.Y. and Hu, Z. J., "Fabrication and oxidation resistance of titanium carbide-coated carbon fibres by reacting titanium hydride with carbon fibres in molten salts." *Thin Solid Films*, 2009, 517, 3248-3252.